



Study of the quasi two-dimensional $\text{Co}_x\text{Ni}_{1-x}\text{Ta}_2\text{O}_6$ compounds by X-ray diffraction and magnetic susceptibility measurements

S.R. de Oliveira Neto ^{a,d,*}, E.J. Kinast ^{b,d}, M.A. Gusmão ^c, C.A. dos Santos ^c, O. Isnard ^d, J.B.M. da Cunha ^c

^a Departamento de Física, Universidade Federal de Sergipe, 49100-000 São Cristóvão, Brazil

^b Universidade Estadual do Rio Grande do Sul, Rua 7 de Setembro, 1156, 90010-191 Porto Alegre, Brazil

^c Instituto de Física, Universidade Federal do Rio Grande do Sul, C.P. 15051, 91501-970 Porto Alegre, Brazil

^d Institut Néel, CNRS/ Université J. Fourier, B.P. 166, 38042 Grenoble Cedex 9, France

ARTICLE INFO

Article history:

Received 27 January 2012

Received in revised form

20 March 2012

Available online 31 May 2012

Keywords:

$\text{Co}_x\text{Ni}_{1-x}\text{Ta}_2\text{O}_6$ series

X-ray powder diffraction

Magnetic susceptibility

Broadened maximum

Ion anisotropy

Two dimensional AF ordering

ABSTRACT

We report results on the structural and magnetic properties of the $\text{Co}_x\text{Ni}_{1-x}\text{Ta}_2\text{O}_6$ series of compounds by X-ray powder diffraction, magnetic susceptibility and magnetization measurements. X-ray refinements carried out by the Rietveld method show that these compounds crystallize in a $P4_2/mnm$ tetragonal structure. Magnetic susceptibility curves show a broadened maximum witnessing that these compounds exhibit two-dimensional antiferromagnetic behaviors. All the $\text{Co}_x\text{Ni}_{1-x}\text{Ta}_2\text{O}_6$ compounds order below 10 K and present a large ion anisotropy. The magnetic properties have been determined in both the paramagnetic and antiferromagnetic state. In the hypothesis of two dimensional AF ordering, the near neighbor exchange constants (J_1) and the next near neighbor exchange constants for two different paths (J_2 and J'_2) were determined. The composition dependence of the magnetic properties including ordering temperature, exchange constants and anisotropy factors are discussed. The drastic reduction of the ordering temperature for $x=0.20$ for $\text{Co}_x\text{Ni}_{1-x}\text{Ta}_2\text{O}_6$, suggest the hypothesis of a peculiar magnetic behavior for this composition.

© 2012 Elsevier B.V. All rights reserved.

1. Introduction

The antiferromagnetic compounds ATa_2O_6 , where $A=\text{Fe}, \text{Co}$ or Ni , have been studied for several years [1–4]. These oxides crystallize in the trirutile structure with space group $P4_2/mnm$ (136). In this structure, A^{2+} and Ta^{5+} cations are surrounded by O^{2-} octahedra. These compounds have been reported to present low-dimensional magnetic character due to pairs of $\text{Ta}-\text{O}$ (at $z=1/6$ and $z=1/3$) planes that separate those containing the 3d transition-metal ions (at $z=0$ and $z=1/2$). Even though the family of compounds shares the crystal structure, different magnetic structures are observed for different 3d ions. Nevertheless, all these compounds present uniaxial anisotropy rotated by 90° with respect to neighbor. The anisotropy field direction, on the basal plane, correlates with the symmetry of the local field originating from the oxygen atoms belonging to the A^{2+} cations' coordination in the lattice.

Neutron diffraction measurements revealed magnetic structures with double propagation vectors: $(\frac{1}{2}, 0, \frac{1}{2})$ and $(0, \frac{1}{2}, \frac{1}{2})$ for FeTa_2O_6 [5]; $(\pm \frac{1}{4}, \frac{1}{4}, \frac{1}{4})$ for CoTa_2O_6 [6]; and $(\pm \frac{1}{4}, \frac{1}{4}, \frac{1}{2})$ for

NiTa_2O_6 [7]. The complex behaviors of these magnetic compounds have attracted much interest leading recently to investigation of the properties of the mixed $\text{Fe}_x\text{Co}_{1-x}\text{Ta}_2\text{O}_6$ and $\text{Fe}_x\text{Ni}_{1-x}\text{Ta}_2\text{O}_6$ oxides. Studies of structural and magnetic properties of substituted compounds have already been reported for $\text{Fe}_x\text{Co}_{1-x}\text{Ta}_2\text{O}_6$ and $\text{Fe}_x\text{Ni}_{1-x}\text{Ta}_2\text{O}_6$ [8,9,20].

In the present work, we focus our attention on the investigation of the structural and magnetic properties of the $\text{Co}_x\text{Ni}_{1-x}\text{Ta}_2\text{O}_6$ samples for $x=0.0, 0.2, 0.4, 0.6, 0.8$ and 1.0 using X-ray diffraction, magnetic susceptibility and magnetization measurements. This article is organized as follows, after a description on the experimental methods used in Section 2, we will successively present and discuss the structural and magnetic results in Section 3, and finally conclusions in Section 4 are given.

2. Experimental and methods

2.1. Synthesis

To investigate this possibility we report, in the present work, the synthesis and investigation of $\text{Co}_x\text{Ni}_{1-x}\text{Ta}_2\text{O}_6$ samples for $x=0.0, 0.2, 0.4, 0.6, 0.8$ and 1.0 by X-ray diffraction, magnetic susceptibility and magnetization measurements. We have prepared powder $\text{Co}_x\text{Ni}_{1-x}\text{Ta}_2\text{O}_6$ samples from precursors CoTa_2O_6

* Corresponding author at: Departamento de Física, Universidade Federal de Sergipe, 49100-000 São Cristóvão, Brazil.

E-mail address: sroneto@ufs.br (S.R. de Oliveira Neto).

and NiTa_2O_6 . Both CoTa_2O_6 and NiTa_2O_6 were prepared in air by the solid state reaction of Co_3O_4 and Ta_2O_5 for the first compound, and NiO and Ta_2O_5 for the second. For each compound, appropriate amounts of the powdered reactants were mixed, ground, pressed to pellets and heat treated in air at 1400 K for CoTa_2O_6 and at 1600 K for NiTa_2O_6 for 30 h with an intermediate regrinding after 24 h. Then, they were slowly cooled and powdered down to a maximum grain size of about 40 μm . For $\text{Co}_x\text{Ni}_{1-x}\text{Ta}_2\text{O}_6$ samples, appropriate amounts of CoTa_2O_6 and NiTa_2O_6 were mixed and processed as for the NiTa_2O_6 preparation. The samples have been found to be stable in air at ambient condition since the X-ray pattern has been found to be identical after several months.

2.2. X-ray powder diffraction

The sample purity was first checked by X-ray diffraction (XRD) analysis before carrying magnetic susceptibility, and magnetization measurements [8]. Such XRD analysis has been performed with a Siemens D5000 diffractometer in Bragg–Brentano geometry installed at the Institut Néel/CNRS, using $\text{CuK}\alpha$ radiation, $\lambda(\text{K}\alpha_1)=1.54056 \text{ \AA}$ with a scan step 0.016° and angular 2θ range from 10° to 80° . The lattice parameters as well as atomic coordinates have been extracted from Rietveld refinement.

2.3. Magnetic measurements

The magnetic measurements have been undertaken on powder sample in a wide temperature range from 1.5 K to 300 K. The measurements have been carried out using the extraction method and an experimental set up that has been described elsewhere [10]. Both isothermal magnetization measurements and temperature dependence of the susceptibility have been performed. The isothermal magnetization curves have been recorded in magnetic field ranging from 0 to 10 T, whereas the magnetic susceptibility was measured in a field of 0.5 T. To assess $\chi(T)$ a constant magnetic field $H=0.5 \text{ T}$ was applied in the field-cooled state in the range 1.5–50 K. To extract information about exchange constants and anisotropy strength, the susceptibility data from room temperature almost down to T_N was comparatively fitted to high-temperature series expansions for both an anisotropic Heisenberg model and an Ising model with competing exchange interactions. For the Ni^{2+} and Co^{2+} cations, surrounded by oxygen atoms in octahedral symmetry, the spin state considered was $S=1$ and $3/2$ respectively.

3. Results

3.1. Crystal structure

At room temperature, narrow X-ray lines ensure that the samples are homogeneous and single-phase and the structure refinement, carried out by the Rietveld method through program FullProf [13], confirms that the samples are well crystallized. A typical pattern is shown in Fig. 1, for $\text{Co}_x\text{Ni}_{1-x}\text{Ta}_2\text{O}_6$.

In such tetragonal type structure, the Ni^{2+} or Co^{2+} cations are located at the corners and in the middle of the unit cell, at the (000) and $(\frac{1}{2} \frac{1}{2} \frac{1}{2})$ positions. The layers of these cations are separated by two layers of Ta^{5+} , at the position $z \sim 1/6$ and $z \sim 1/3$. The O^{2-} are placed surrounding the cations shaping octahedrons. It was shown in a previous work [5,11], that the oxygen octahedrons surrounding the Ni^{2+} (or Co^{2+}) are rotated by 90° for a translation of $(\frac{1}{2} \frac{1}{2} \frac{1}{2})$. Fig. 2 presents the crystal structure of the $\text{Co}_x\text{Ni}_{1-x}\text{Ta}_2\text{O}_6$ compounds and illustrates the tilt of the octahedron.

According to the Rietveld analysis, the lattice parameters are significantly affected by the Co for Ni substitution. Fig. 3 presents

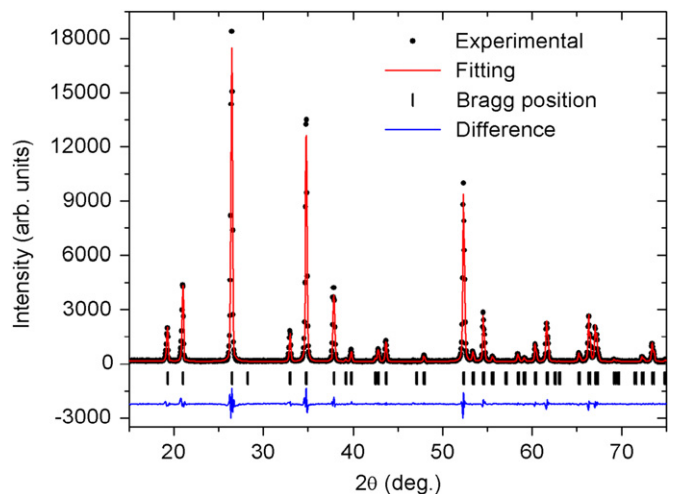


Fig. 1. Room temperature X-ray powder diffraction pattern for $\text{Co}_{0.80}\text{Ni}_{0.20}\text{Ta}_2\text{O}_6$.

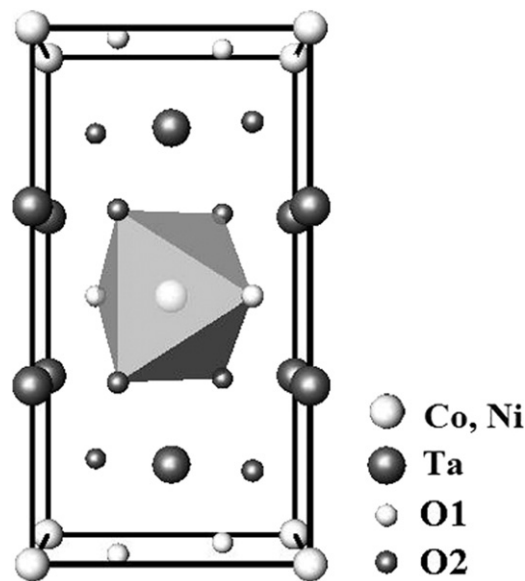


Fig. 2. Crystal structure of the trirutile unit cell for $\text{Co}_x\text{Ni}_{1-x}\text{Ta}_2\text{O}_6$.

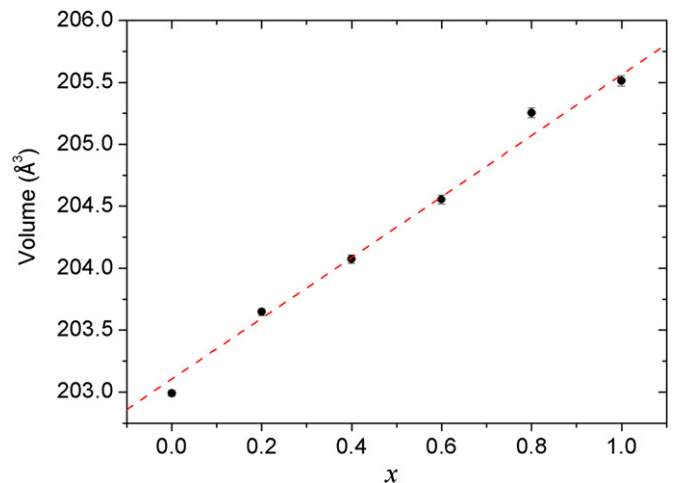


Fig. 3. Variations in the unit cell volume as a function of cobalt concentration. The solid line is a linear fit of the experimental data.

Table 1
Lattice parameters, c/a ratio and unit-cell volume of the $\text{Co}_x\text{Ni}_{1-x}\text{Ta}_2\text{O}_6$.

Sample	a (Å)	c (Å)	c/a	Volume (Å ³)
NiTa ₂ O ₆	4.7168 (3)	9.1238 (7)	1.9343	203.0
Co _{0.20} Ni _{0.80} Ta ₂ O ₆	4.7213 (3)	9.1356 (8)	1.9349	203.6
Co _{0.40} Ni _{0.60} Ta ₂ O ₆	4.7246 (4)	9.142 (1)	1.9349	204.0
Co _{0.60} Ni _{0.40} Ta ₂ O ₆	4.7278 (4)	9.152 (1)	1.9358	204.5
Co _{0.80} Ni _{0.20} Ta ₂ O ₆	4.7326 (4)	9.164 (1)	1.9364	205.2
CoTa ₂ O ₆	4.7342 (5)	9.1693 (13)	1.9368	205.5

Table 2
Interatomic distances between transition metal ion (Co/Ni) and neighboring oxygen and distortion index DI of the corresponding distorted octahedra for $\text{Co}_x\text{Ni}_{1-x}\text{Ta}_2\text{O}_6$.

Sample	$\overline{\text{AO1}}$ (Å)	$\overline{\text{AO2}}$ (Å)	$\langle \overline{\text{AOi}} \rangle$ (Å)	DI (%)
NiTa ₂ O ₆	2.0810	2.1413	2.1111	2.8
Co _{0.20} Ni _{0.80} Ta ₂ O ₆	2.0496	2.1697	2.1096	5.7
Co _{0.40} Ni _{0.60} Ta ₂ O ₆	2.1074	2.1766	2.1420	3.2
Co _{0.60} Ni _{0.40} Ta ₂ O ₆	2.0669	2.1664	2.1167	4.7
Co _{0.80} Ni _{0.20} Ta ₂ O ₆	2.0937	2.2144	2.1540	5.6
CoTa ₂ O ₆	2.1881	2.2555	2.2218	3.0

the unit cell volume as a function of x . This clearly shows the continuous evolution of the unit cell volume versus the cobalt content following Vegard's Law. The evolution of the corresponding a and c lattice parameters, c/a ratio and volume are summarized in Table 1. It is worth to note that the unit-cell parameters as well as the volume increase as the cobalt concentration. A slight anisotropic expansion occurs since the c/a ratio evolves continuously along the series. This increase is due to the larger expansion along the c axis.

The distortion index (DI) of the oxygen octahedron [8] remains positive whatever the concentration as can be seen from Table 2. The DI is defined as

$$DI = \frac{\overline{\text{AO2}} - \overline{\text{AO1}}}{\langle \overline{\text{AOi}} \rangle} \quad (1)$$

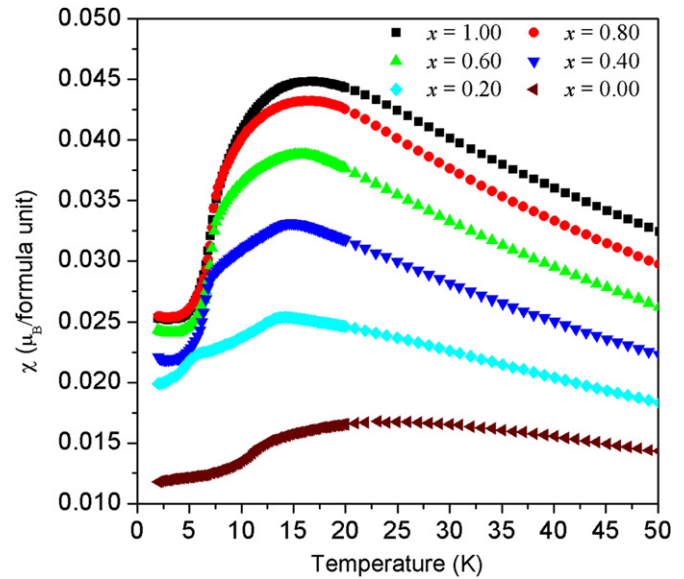
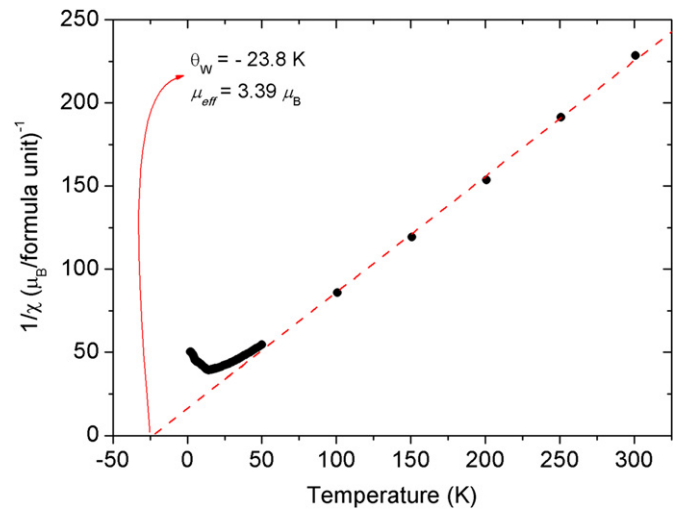
where $\text{AO1}(2)$ is the distance between Ni/Co atoms and the O1(2) oxygen and AOi is the mean semi-diagonal [14]. This positive value reflects that the Ni/Co octahedral are elongated along one direction corresponding to the O2. Such distortion is expected to have a significant influence on the local crystal electric field experienced at the Ni/Co crystal site and consequently on the magnetic anisotropy of the ions. The present results demonstrate that the distortion index remains of the same sign and order of magnitude whatever the composition thus keeping a large magnetocrystalline anisotropy.

3.2. Magnetic measurements

As can be seen from Fig. 4, the thermal dependence of the magnetic susceptibility is not that of a simple antiferromagnet structure. Above the ordering temperature the susceptibility χ is following Curie-Weiss law

$$\frac{1}{\chi} = \frac{T - \Theta_W}{C} \quad (2)$$

The corresponding parameters C and Θ_W , obtained from the fit of the high temperature ($T > 100$ K), as shown on the Fig. 5 for $\text{Co}_{0.20}\text{Ni}_{0.80}\text{Ta}_2\text{O}_6$, are listed in Table 3. At low temperature a broad peak is observed in the susceptibility, a feature reported for compounds exhibiting two dimensional magnetic character. The

**Fig. 4.** Magnetic susceptibility data for $\text{Co}_x\text{Ni}_{1-x}\text{Ta}_2\text{O}_6$ measured at 5 kOe.**Fig. 5.** Curie-Weiss law fit to the magnetic susceptibility data for $\text{Co}_{0.20}\text{Ni}_{0.80}\text{Ta}_2\text{O}_6$.**Table 3**

Curie-Weiss temperature Θ_W , Curie constant C , effective magnetic moment μ_{eff} , Landé g -factor and Néel temperature obtained experimentally for the $\text{Co}_x\text{Ni}_{1-x}\text{Ta}_2\text{O}_6$ series of compounds. The estimation of the Landé factor has been deduced assuming $\mu_{\text{eff}} = g(S(S+1))^{1/2}$.

Sample ATa ₂ O ₆	Θ_W (K)	C (emu K/mol/Oe)	μ_{eff} (μ _B)/A	g	T_N (K)
NiTa ₂ O ₆	-19.9 (1.7)	1.11 (3)	2.97 (4)	2.10 (3)	11.2 (3)
Co _{0.20} Ni _{0.80} Ta ₂ O ₆	-23.8 (3.7)	1.44 (3)	3.39 (4)	2.23 (2)	5.0 (3)
Co _{0.40} Ni _{0.60} Ta ₂ O ₆	-23.1 (3.2)	1.72 (3)	3.71 (3)	2.28 (2)	6.6 (3)
Co _{0.60} Ni _{0.40} Ta ₂ O ₆	-24.8 (3.2)	2.07 (4)	4.07 (4)	2.35 (2)	7.2 (3)
Co _{0.80} Ni _{0.20} Ta ₂ O ₆	-22.1 (4.4)	2.29 (7)	4.28 (6)	2.34 (3)	7.2 (3)
CoTa ₂ O ₆	-29.6 (3.9)	2.72 (5)	4.67 (5)	2.41 (2)	7.0 (3)

ordering temperature has been determined from the first derivative of the magnetic susceptibility [17], recorded in the range from 1.5 to 20 K. Such approach has been shown to be appropriate for two dimensional systems. In order to have a precise determination of the Néel temperature T_N , the magnetic susceptibility has

been measured every 0.2 K. As can be seen from Fig. 6, which presents the magnetic contribution to the specific heat for $x=0.20, 0.40$ and 0.60 , $d(\chi T)/dT$ is characterized by a λ -shaped anomaly indicating magnetic ordering.

It is interesting to remark that the Néel temperatures T_N listed in Table 3 are much smaller than the paramagnetic temperature Θ_W . The ratio Θ_W/T_N is often referred to as frustration parameter indicating of magnetic frustration when this ratio differs significantly from unity. For the $\text{Co}_x\text{Ni}_{1-x}\text{Ta}_2\text{O}_6$ compounds studied here, the Θ_W/T_N ratio is slightly below 5 and typically ranging from 3.7 up to 4.5. These values are close to 5 a value usually taken as a reference for the presence of magnetic frustration [18,19]. This may be taken as an indication of the presence of competing exchange interactions in these compounds. In order to go deeper into the analysis of such possible frustration, it would be interesting to know the precise magnetic structure of these compounds as well as the magnitude of the magnetic interactions between all the neighbors. It is clearly seen that Co for Ni partial substitutions leads to a significant reduction of the Curie–Weiss temperature in respect to the beginning or end of the $\text{Co}_x\text{Ni}_{1-x}\text{Ta}_2\text{O}_6$ series. This large decrease reflects the reduction of the negative character of the overall exchange interactions when cobalt and nickel share the crystal structure. This may also be interpreted as an effect of the chemical disorder on the magnetic interactions.

The presence of a minimum of T_N at $x=0.20$ may be indicative of a different magnetic behavior. Indeed unusual bicriticality and coexistence of magnetic structures has been reported for similar lowering of the Néel temperature in the isotype $\text{Fe}_x\text{Co}_{1-x}\text{Ta}_2\text{O}_6$ and $\text{Fe}_x\text{Ni}_{1-x}\text{Ta}_2\text{O}_6$ systems [11,20,21].

The present results for CoTa_2O_6 and NiTa_2O_6 are shown in Table 4 and are compared with those of Takano and Takada [1]

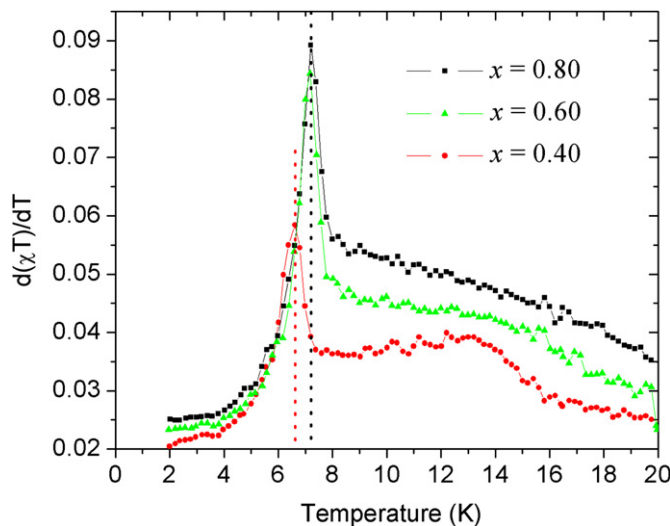


Fig. 6. Contribution to the heat capacity as obtained from susceptibility [17] data for $\text{Co}_x\text{Ni}_{1-x}\text{Ta}_2\text{O}_6$ series showing a λ -type anomaly.

and Bernier and Poix [15]. Our parameters are somewhat different than those of these authors, but it is clear that agreement is generally good among the three studies.

The determination of the Curie–Weiss constant reveals an increase of the paramagnetic effective moment upon increasing the Co concentration—see Fig. 7. This is not surprising since the Co^{2+} ion is expected to exhibit a slightly larger effective magnetic moment than Ni^{2+} : 6.63 and $5.59 \mu_B$ respectively [16,22].

The effective magnetic moments obtained here for the $\text{Co}_x\text{Ni}_{1-x}\text{Ta}_2\text{O}_6$ series are significantly larger than the value expected for orbital quenching ($L=0$) of the transition metal ions 3.87 and $2.83 \mu_B$ for Co^{2+} than Ni^{2+} respectively. This proves that the orbital moment is not completely quenched. One can consequently expect a Landé factor value unequal to 2. This conclusion is in agreement with the results given in Table 3 where values of g ranging from 2.1 to 2.4 are obtained experimentally.

Fig. 8 shows the magnetic phase diagram for the whole $\text{Co}_x\text{Ni}_{1-x}\text{Ta}_2\text{O}_6$ series, the Néel temperature is always below 11 K throughout the series, but with marked sudden reduction again for the sample $x=0.20$. It has been seen, for the $\text{Fe}_x\text{Co}_{1-x}\text{Ta}_2\text{O}_6$ series, that for the concentration exhibiting the minimum value of the Néel temperature versus the x phase diagram corresponds to the same one that it presents the phenomenon of the coexistence: $x=0.46$ [11]. A similar correspondence was discovered for $\text{Fe}_x\text{Ni}_{1-x}\text{Ta}_2\text{O}_6$ structure [20].

In order to probe the exchange interactions involved in this family of compounds, a fit of the susceptibility has been carried out in the range from 15 to 300 K using the Hamiltonian proposed

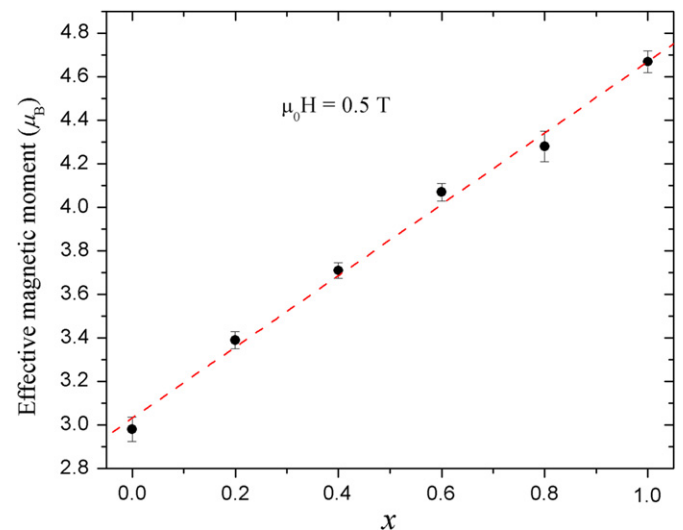


Fig. 7. Variation of the high-temperature effective magnetic moment as a function of concentration along the $\text{Co}_x\text{Ni}_{1-x}\text{Ta}_2\text{O}_6$ series. Solid points are the data obtained from magnetic susceptibility measurements. The dotted line is a guide to the eyes.

Table 4

Comparison of data and magnetic parameters of this work and Takano and Takada [1] and Bernier and Poix [15].

	This work		Takano and Takada[1]		Bernier and Poix[15]	
	CoTa_2O_6	NiTa_2O_6	CoTa_2O_6	NiTa_2O_6	CoTa_2O_6	NiTa_2O_6
$T(\chi_{\text{max}})$ (K)	16.72	23.09	16	26	15	23
$\chi_{\text{max}} (\times 10^{-2} \text{ emu})$	4.486	1.678	4.63	1.71	4.855	1.698
Θ_W (K)	−29.6	−19.9	−35	−41	−27	−50
C ($\text{cm}^3 \text{ K/mol}$)	2.72	1.11	3.53	2.1	3	1.43
μ_{eff} (μ_B)	4.67	2.97	5.31	4.1	4.9	3.38

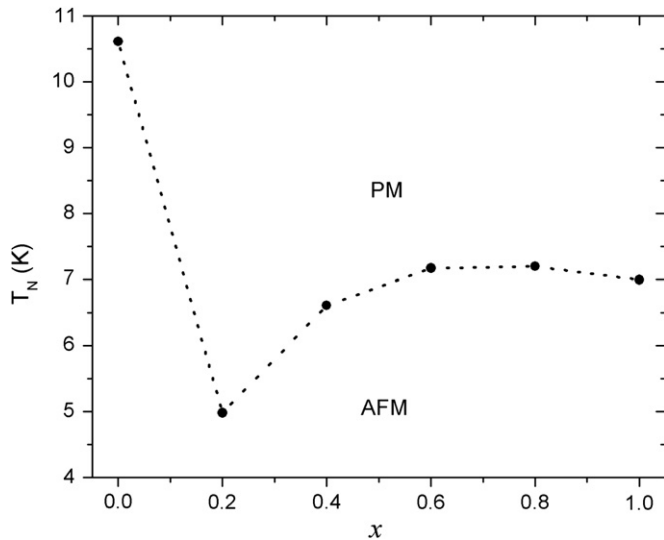


Fig. 8. Composition by dependence of the ordering temperature of the $\text{Co}_x\text{Ni}_{1-x}\text{Ta}_2\text{O}_6$ series, showing the paramagnetic (PM) and antiferromagnetic (AFM) regions. Solid points are the Néel Temperature values obtained from magnetic susceptibility measurements. Dot lines are guide to the eyes.

by Muraoka et al. [12]

$$H = -2J_1 \sum_{\langle ij \rangle} \vec{S}_i \vec{S}_j - 2\alpha J_1 \sum_{\langle\langle ij \rangle\rangle} \vec{S}_i \vec{S}_j - D \sum_i S_{iz}^2 - \mu_B h \sum_i (g_{\parallel} S_{iz} + g_{\perp} S_{ix}) \quad (3)$$

where the first two terms represent respectively the exchange interactions of Heisenberg type with the first (nm) and second (nnn) nearest neighbors carrying a spin of \vec{S}_i and \vec{S}_j , J_1 and J_2 being the exchange constants to the first and second nearest neighbors. The possible exchange interaction paths between the magnetic cations are sketched in Fig. 9. For simplicity, a mean J_2 value has been refined in spite of the possibility for the two inequivalent exchange paths.

The third term describes the anisotropy of the $\text{Ni}^{2+}/\text{Co}^{2+}$ ions along the principal axis of the distorted octahedral z , that is to say along the Co–O1 direction. D is the anisotropy coefficient. The last term represents the Zeemann effect where g_{\parallel} and g_{\perp} are the Landé factors respectively parallel and perpendicular to the local z^* principal axis. For more details, the reader is referred to the publication of Muraoka et al. [12].

Fig. 10 shows the fit (red line) for the high-temperature data points from magnetic susceptibility measurements for $\text{Co}_{0.40}\text{Ni}_{0.60}\text{Ta}_2\text{O}_6$. The refined magnetic parameters obtained from the fit of the thermal evolution of the susceptibility in the paramagnetic regime are listed in Table 5. However, some inconsistencies can be seen in this table concerning the parameters related to the magnetic anisotropy, D and $\langle g \rangle$. These parameters present developments in opposite directions, not allowing a reasonable conclusion about the evolution of anisotropy in range $0.0 < x < 1.0$. In addition, the difference between the values of g_{\parallel} and g_{\perp} are also reduced as D increases, and the values of $\langle g \rangle$ in Table 5 are not consistent with those obtained from the Curie–Weiss fitting (Table 3).

We believe that these inconsistencies and the high values of D are caused by an excessive number of parameters to be adjusted with the known coefficients of the high-temperature series, allowing several different configurations with similar adjustments. Furthermore, this model does not take into account the two distinct paths of interaction between next-nearest neighbors J_2 and J'_2 .

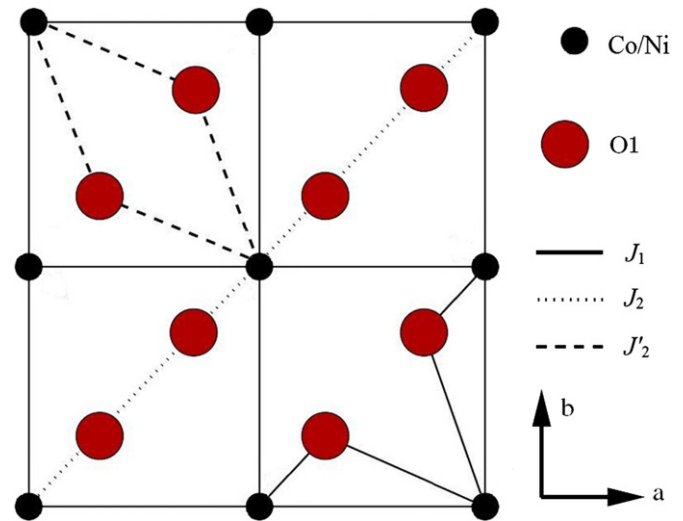


Fig. 9. Superexchange paths between nearest- and next-nearest-neighbors on a magnetic ab plane (adapted from Ref. 4). The dotted and dashed lines represent two possible paths for J_2 . The indicated exchange constants follow the notation appearing in the models that we used.

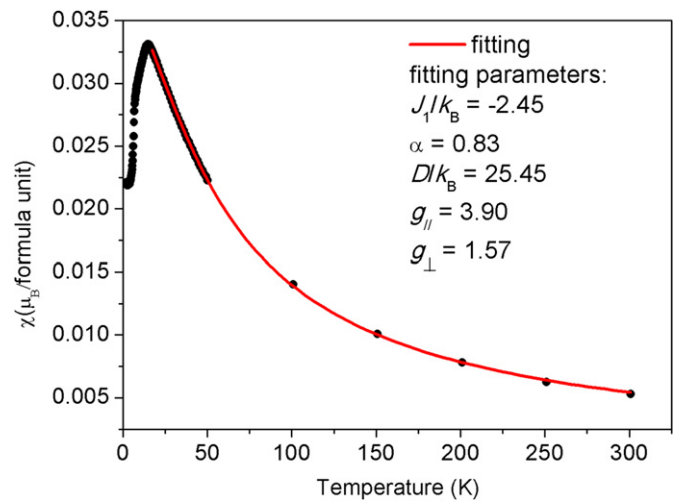


Fig. 10. Magnetic susceptibility fitting for $\text{Co}_{0.40}\text{Ni}_{0.60}\text{Ta}_2\text{O}_6$ by the method of high-temperature series. (For interpretation of the references to colour in this figure, the reader is referred to the web version of this article.)

An alternative Ising model was proposed for the isotype compounds $\text{Fe}_x\text{Co}_{1-x}\text{Ta}_2\text{O}_6$ by Santos et al. [20], defined by the Hamiltonian

$$H = -2J_1 \sum_{\langle ij \rangle} S_i^z S_j^z - 2J_2 \sum_{\langle\langle ij \rangle\rangle} S_i^z S_j^z - 2J'_2 \sum_{\langle\langle ij \rangle\rangle} S_i^z S_j^z - gH_z \sum_i S_i^z \quad (4)$$

where \parallel and \perp are relative to the anisotropy axis. The fit of this model provide us results more consistent as shown in Table 6 for the values of the J_1, J_2, J'_2 and $\langle J_2 \rangle$. The obtained values of J_2 and J'_2 are consistent with a planar spin structure in which the alignment is antiferromagnetic along the path of J_2 and ferromagnetic along that of J'_2 . For instance, this is what is observed for Co-rich compounds in the $\text{Fe}_x\text{Co}_{1-x}\text{Ta}_2\text{O}_6$ series [20].

Fig. 11 shows the variation of the J_1, J_2, J'_2 and $\langle J_2 \rangle$ exchange interactions in range $0.0 < x < 1.0$. We note that at $x=0.20$ there is a sudden change in J_1 and J_2 so that their intensities become closer. This abrupt change in J_1 and J_2 was also observed in

Table 5
Magnetic parameters refined from the fit of the high temperature susceptibility following the Heisenberg model [12]. J_1 and J_2 refer to the near and next near neighbor exchange constants, $\alpha = J_2/J_1$, D is the magnetic anisotropy parameter, g_{\parallel} and g_{\perp} correspond to the longitudinal and transverse components of the Lande factor of the Co^{2+} or Ni^{2+} ions sitting in the distorted octaheda. The typical standards deviations are indicated in parenthesis in the first row.

Sample	J_1/k_B (K)	J_2/k_B (K)	α	D/k_B (K)	g_{\parallel}	g_{\perp}	$\langle g \rangle$
NiTa ₂ O ₆	-3.41(10)	-3.48(10)	1.02(2)	56.7(1)	3.51	2.03	3.08
Co _{0.20} Ni _{0.80} Ta ₂ O ₆	-2.57	-2.57	1.00	34.2	3.67	1.70	3.01
Co _{0.40} Ni _{0.60} Ta ₂ O ₆	-2.45	-2.04	0.83	25.4	3.90	1.57	3.12
Co _{0.60} Ni _{0.40} Ta ₂ O ₆	-2.30	-1.83	0.80	21.4	4.09	1.49	3.22
Co _{0.80} Ni _{0.20} Ta ₂ O ₆	-1.95	-1.69	0.86	18.3	4.12	1.42	3.22
CoTa ₂ O ₆	-1.60	-1.98	1.23	17.9	4.20	1.37	3.25

Table 6
Exchange constants refined from the fit of the high temperature susceptibility following the Ising model (4). J_1 refer to the near neighbor exchange constants while J_2 and J'_2 refer to next near neighbor exchange constants for two different paths.

Sample	J_1/k_B (K)	J_2/k_B (K)	J'_2/k_B (K)	$\langle J_2 \rangle/k_B$ (K)
NiTa ₂ O ₆	-0.110	-6.14	0.126	-3.01
Co _{0.20} Ni _{0.80} Ta ₂ O ₆	-1.110	-3.95	0.298	-1.83
Co _{0.40} Ni _{0.60} Ta ₂ O ₆	-0.145	-3.99	0.530	-1.73
Co _{0.60} Ni _{0.40} Ta ₂ O ₆	-0.220	-3.45	0.451	-1.50
Co _{0.80} Ni _{0.20} Ta ₂ O ₆	-0.136	-3.21	0.777	-1.22
CoTa ₂ O ₆	-0.452	-2.63	0.237	-1.20

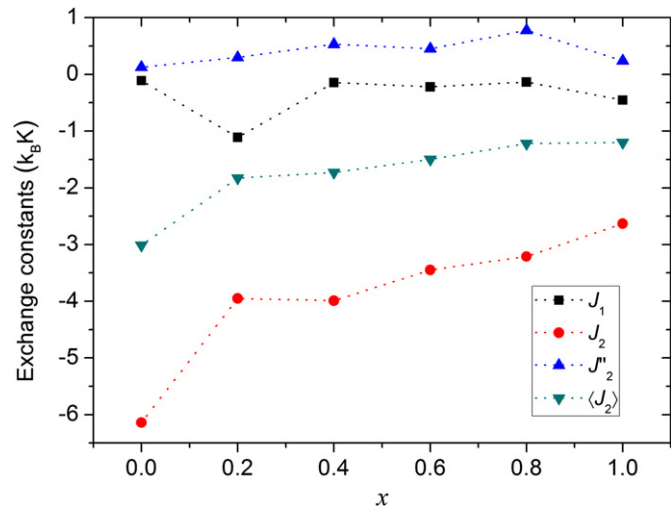


Fig. 11. Exchange constants of the Ising model (4) for varying x values throughout the $\text{Co}_x\text{Ni}_{1-x}\text{Ta}_2\text{O}_6$ series, as obtained from fittings of the susceptibility data to the corresponding high-temperature series.

$\text{Fe}_x\text{Co}_{1-x}\text{Ta}_2\text{O}_6$ at concentrations close to those which were determined magnetic phase coexistence [20].

Following this interpretation, a coexistence of magnetic phase could be expected for $x=0.20$ in the $\text{Co}_x\text{Ni}_{1-x}\text{Ta}_2\text{O}_6$ series. The particularly low value of the Néel temperature obtained for $x=0.20$ composition may result from competition between exchange interactions. It is worth noting that the minimum of T_N value observed here for the $\text{Co}_x\text{Ni}_{1-x}\text{Ta}_2\text{O}_6$ compounds is precisely obtained for the $x=0.20$ composition. Further studies are necessary to clarify this possible correspondence.

This simple reasoning on the basis of the fit of our experimental results demonstrates that there is competing exchange interactions in the whole $\text{Co}_x\text{Ni}_{1-x}\text{Ta}_2\text{O}_6$ series of compounds. This confirms the clues for frustration derived from the Θ_W/T_N ratio as discussed above.

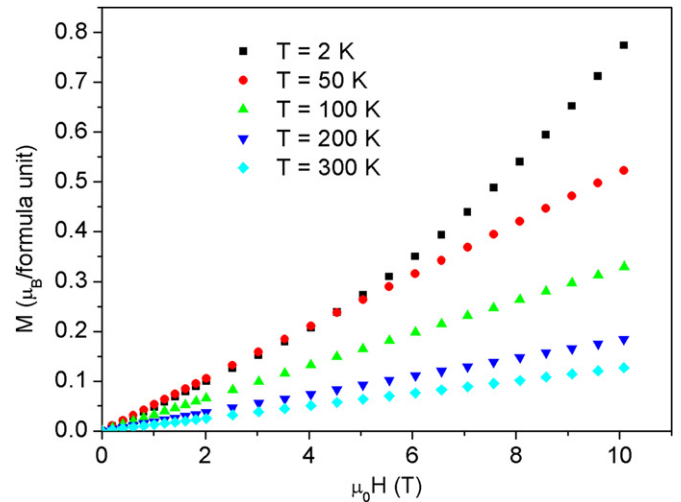


Fig. 12. Magnetization versus applied field for various temperatures for $\text{Co}_{0.60}\text{Ni}_{0.40}\text{Ta}_2\text{O}_6$.

As can be seen from Fig. 12, the magnetization curves recorded above the T_N for $\text{Co}_{0.6}\text{Ni}_{0.4}\text{Ta}_2\text{O}_6$ are, as expected, linear. Below T_N two regimes are observed first a linear behavior with a slope comparable to that observed at high temperature, then an upturn occurs with a change of slope. This sudden change in the $M \times H$ curve at the field for which a spin-flop transition occurs can be taken as an experimental signature of easy-axis magnetic anisotropy [22], thus confirming the large anisotropy parameters derives from the high temperature fit of the magnetic susceptibility. This change of slope in the magnetization curve can be observed in Fig. 12 for magnetization curves recorded on powder sample. Although not as pronounced as one would have for a single-crystal sample, the low-temperature curve presents a clear change in slope around $\mu_0 H = 6$ T for $\text{Co}_{0.6}\text{Ni}_{0.4}\text{Ta}_2\text{O}_6$. This relatively high critical field confirms that the anisotropy is strong. It is worth to notice that a critical field of similar magnitude has been reported for a single crystal of the isotype compound FeTa_2O_6 [4] or polycrystalline CoTa_2O_6 [23]. It is worth to note that no sign of saturation can be observed up to 10 T meaning that the field necessary to obtain a ferromagnetic alignment of the magnetic moment is much larger than 10 T.

4. Conclusions

By a systematic study of the $\text{Co}_x\text{Ni}_{1-x}\text{Ta}_2\text{O}_6$ series of compounds, we have shown that they crystallize in a $P4_2/mnm$ tetragonal structure and confirms the existence of a complete solid solution. According to the magnetic measurements, these compounds exhibit two dimensional antiferromagnetic behaviors. Due to the contradictory correspondence between D and $\langle g \rangle$ values obtained from the model proposed by Muraoka, we used

the Ising model introduced in Ref. [20], which takes into account the two distinct pathways of exchange interactions between the next nearest neighbors. The J_2 and J'_2 values indicate that the magnetic moments align ferromagnetically along one direction and antiferromagnetically in the direction transverse to that.

The lower Néel temperature has been observed for $x=0.20$, a composition exhibiting also a more pronounced competition between the J_1 and J_2 values. Similar behavior occurring in $\text{Fe}_x\text{Co}_{1-x}\text{Ta}_2\text{O}_6$ around concentrations of coexisting magnetic phases motivates a more detailed study of these composition regions in a forthcoming investigation. Further investigation by neutron diffraction is necessary to determine the magnetic structures of these compounds below the ordering temperature.

Acknowledgments

This work was supported in part by the French–Brazilian CAPES-COFECUB cooperation program No. 600/08. The Brazilian agencies CNPq are also warmly acknowledged. S.R. de Oliveira Neto and O. Isnard, on behalf of the University Joseph Fourier, are thankful to the Region Rhône Alpes, France, for invaluable support in the frame of the ARCUS-Bresil program.

References

- [1] M. Takano, T. Takada, *Materials Research Bulletin* 5 (1970) 449.
- [2] R.K. Kremer, J.E. Greedan, E. Gmelin, W. Dai, M.A. White, S.M. Eicher, K.J. Lushington, *Journal de Physique Colloques* 49 (C8) (1988) 1495–1496.
- [3] L.I. Zawislak, J.B.M. da Cunha, A. Vasquez, C.A. dos Santos, *Solid State Communications* 94 (1995) 345–348.
- [4] E.M.L. Chung, M.R. Lees, G.J. McIntyre, C. Wilkinson, G. Balakrishnan, J.P. Hague, D. Visser, D.McK Paul, *Journal of Physics: Condensed Matter* 16 (2004) 7837.
- [5] S.M. Eicher, J.E. Greedan, K.J. Lushington, *Journal of Solid State Chemistry* 62 (1986) 220.
- [6] J.N. Reimers, J.E. Greedan, C.V. Stager, R. Kremer, *Journal of Solid State Chemistry* 83 (1989) 20.
- [7] H. Ehrenberg, G. Wltschek, J. Rodriguez-Carvajal, T. Vogt, *Journal of Magnetism and Magnetic Materials* 184 (1998) 111.
- [8] V. Antonietti, E.J. Kinast, L.I. Zawislak, J.B.M. da Cunha, C.A. dos Santos, *Journal of Physics and Chemistry of Solids* 62 (2001) 1239.
- [9] S.R.O. Neto, E.J. Kinast, M.A. Gusmão, C.A. dos Santos, O. Isnard, J.B.M. da Cunha, *Journal of Physics: Condensed Matter* 19 (2007) 356210.
- [10] A. Barlet, J.C. Genna, P. Lethuillier, *Cryogenic* 31 (1991) 801.
- [11] E.J. Kinast, V. Antonietti, D. Schmitt, O. Isnard, J.B.M. da Cunha, M.A. Gusmão, C.A. dos Santos, *Physical Review Letters* 91 (2003) 19720.
- [12] Y. Muraoka, T. Idogaki, N. Uryu, *Journal of the Physical Society of Japan* 57 (1988) 1758.
- [13] J. Rodriguez-Carvajal, *Physica B* 192 (1993) 55.
- [14] M. Saes, N.P. Raju, J.E. Greedan, *Journal of Solid State Chemistry* 140 (1998) 7.
- [15] J.C. Bernier, P. Poix, *Annali di Chimica* 3 (1968) 119.
- [16] D. Gignoux, M. Schlenker, *Magnetism I: Fundamentals*, E. du Trémolet de Lacheisserie, Kluwer Academic Press, 2002.
- [17] M.E. Fisher, *Philosophical Magazine* 7 (1962) 1731.
- [18] P. Schiffer, A.P. Ramirez, *Condensed Matter Physics* 18 (1996) 21–50.
- [19] A.P. Ramirez, *Handbook of Magnetic Materials* 13 (2001) 423–520. (Chapter 4).
- [20] E.G. Santos, S.R. de Oliveira Neto, E.J. Kinast, O. Isnard, M.A. Gusmão, J.M.B. da Cunha, *Journal of Physics Condensed Matter* 22 (2010) 496004.
- [21] S.R.O. Neto, E.J. Kinast, M.A. Gusmão, C.A. dos Santos, O. Isnard, J.B.M. da Cunha, *Journal of Magnetism and Magnetic Materials* 320 (2008) e125.
- [22] S. Blundell, *Magnetism in Condensed Matter*, Oxford University Press, 2001.
- [23] E.J. Kinast, C.A. dos Santos, D. Schmitt, O. Isnard, M.A. Gusmão, J.B.M. da Cunha, *Journal of Alloys and Compounds* 491 (2010) 41–44.